MSUCP-16

MICHIGAN STATE UNIVERSITY

CYCLOTRON PROJECT*

Initial Acceleration and Radial Focusing in the Nonuniform Electric Field at the Ion Source of the Cyclotron.

M. Reiser

March 1963

Department of Physics

East Lansing, Michigan

---

*Research Supported in part by The National Science Foundation (Grant NSF-G19978)

Initial Acceleration and Radial Focusing in the Nonuniform Electric Field at the Ion Source of the Cyclotron.*

M. Reiser

Michigan State University
East Lansing, Michigan
March, 1963

ABSTRACT

The electric field in the median plane between ion source and extractor electrode was mapped in a 10:1 scale for various geometric arrangements with the conductivity-paper method. Initial trajectories, energy gain, transit time and radial focusing of the ions in this field region were calculated numerically (neglecting space-charge effects). The calculations disclosed that the nonuniform field produced by the cylindrical arc chamber of the conventional ion source causes a very strong distortion of the radial beam shape. This defocusing effect can be substantially reduced if the arc chamber is flattened at the side facing the extractor electrode to make the field more uniform. Further improvement is possible by recessing the source face at the output slit, in which case a very favorable parallel-beam situation can be achieved. In addition, by proper shaping of the recess, the defocusing effects of space charge and convex plasma boundaries can be balanced out.

*Research supported in part by the National Science Foundation.

1. Introduction.

The insertion of an extractor electrode (or puller) at the dee opposite the ion source is now a generally accepted and widely employed technique of improving ion-source output and cyclotron performance. The technical development from the open-arc source and open-dee geometry of early cyclotrons to the hooded source with "feelers" attached to the dee[1] and finally to the Oak-Ridge type source with extractor electrode[2] of present-day machines was more or less an empirical step-by-step process. Little work in terms of an exact theoretical examination of the optimum source-puller arrangement had been done, mainly because of the complexity of the processes of ion extraction from the arc plasma and subsequent acceleration in the region near the ion source.

During the last few years considerable progress has been made in understanding central-region effects and in improving the starting conditions by programming the beam on its first few turns. Most of this work was based on the uniform-field theory which proved to be extremely helpful in the analysis of energy-time relationships such as energy gain, transit time in the electric-field gaps, radial grouping and phase bunching of ions starting at different phases with respect to the r.f.

---

1) A review of the situation before 1946 is given by M. S. Livingston, Rev. Mod. Phys. 18 (1946), 293.

2) R. S. Livingston and R. J. Jones, Rev. Sci. Instr. 25 (1954), 552.

voltage. The uniform-field model is of course an idealization and for more accurate investigations, particularly for the analysis of radial and vertical focusing, the nonuniformities of both electric and magnetic fields must be taken into account. In this case the actual field distributions have to be either calculated or determined experimentally, and graphical or numerical integration methods must be employed to trace the particle trajectories. While the magnetic field is usually measured in model-magnet setups, the mapping of the electric field configuration can be separated into two regions: (a) the immediate neighborhood of the ion source, where the potential distribution must be determined by electrolytic-tank measurements or other experimental methods, and (b) the region outside the very center, where the distortions produced by ion source, puller and other electrodes have disappeared and the theoretical solutions, derived with the Schwarz-Christoffel method, can be employed[3)4)].

So far only few central-region calculations with nonuniform electric field have been done. Cohen[5)] investigated the electric focusing effects in the Oak-Ridge 86-inch cyclotron by numerical computation of vertical motion using the theoretically derived field configuration of an undistorted, idealized dee geometry.

---

3) R. L. Murray and L. T. Ratner, J. Appl. Phys. 24 (1953), 67.

4) J. W. Beal, MSU-Cyclotron Report 12, Oct., 1961.

5) B. L. Cohen, Rev. Sci. Instr. 24 (1953), 589.

Electrolytic-tank studies of the distorted field region near the ion source were carried out by Panasyuk[6] and Willax[7]. Panasyuk mapped the field in the neighborhood of an open-arc source (which he represented by a metal bar) both in the median plane and in a vertical plane and calculated median-plane trajectories for particles with different starting phases; his investigations led him to the development of a closed arc chamber and an extractor electrode (parallel and similar to the development in Oak Ridge). Willax and Garren measured potential distributions in a vertical plane and median-plane equipotential lines near ion source and puller (in a half-scale mockup of central geometry) for the single-dee arrangement of the Berkeley 88-inch cyclotron. They then calculated the radial motion of the ions by using the uniform-field equations for the region between ion source and puller and by tracing the trajectories in the adjoining region, where the field had been measured, with a graphical integration method.

Electrolytic-tank measurements of median-plane field configurations in a 3:1 scale model of the region near the ion source of the MSU cyclotron with numerical calculations of ion motion are now in progress after a general investigation

---

6) V. S. Panasyuk, Kernenergie 1 (1958), 652.

7) H. A. Willax and A. A. Garren, Nucl. Instr. and Meth. 18-19 (1962), 347.

based on the uniform-field theory provided the necessary guidance and framework for an initial layout[8]. Part of this program is the study of initial acceleration and nonuniform-electric-field effects in the region between ion source and puller, and the results of these studies are presented herein.

2. Geometry and Field Measurements.

The geometric arrangements and shapes of the ion source and extractor electrode differ somewhat from one cyclotron to another. In most cases the arc chamber of the source is a cylindrical structure; in Berkeley[7] and Birmingham[9] the chamber is slightly flattened around the output slit. Morton and Smith[10] used an ion source with rectangular cross section in the Canberra cyclotron to match closely the uniform-field assumptions of the theory and provide better control for centering of the orbits.

The Oak-Ridge type of extractor electrode[2] has a long vertical slit with small radial aperture and has a slight angle in vertical direction to provide some electric focusing for the outermost particles. By contrast, the puller of the Canberra cyclotron has a long horizontal slit with small

---

8) M. Reiser, MSU-Cyclotron Report 15, February, 1963.

9) A. J. Cox, D. E. Kidd, W. B. Powell, B. L. Reece, P. J. Waterton, Nucl. Instr. and Meth. 18-19 (1962), 25.

10) A. H. Morton and W. I. B. Smith, Nucl. Instr. and Meth. 4 (1959), 36.

vertical aperture and only one side bar intercepting the median plane[11]. This puller shape was chosen on the grounds that there is strong vertical focusing by the curved plasma boundary as the ions leave the source and that this effect balances the vertical defocusing due to the puller slit. Besides, a long horizontal slit allows some radial readjustment of the source without changing the puller position. The extractor electrode in the Berkeley 88-inch cyclotron[7] is more or less a compromise between the Oak-Ridge and the Canberra solution; it has a square slit and is curved vertically and radially to provide some focusing field components in both directions.

For the present investigation a puller of the Oak-Ridge type was chosen with a narrow slit whose vertical height is considerably larger than the radial width, and for the ion source both a cylindrical and a square cross section were studied. If the height of the extractor slit is much larger than the slit width and the distance to the ion source, the mapping of the median-plane potential distribution is in good approximation a two-dimensional problem for which the conducting-paper method can be applied.

The geometry for the field measurements is outlined in Fig. 1. The diameter D of the source, the slit width s and thickness b of the puller were fixed parameters with

---

11) W. I. B. Smith, Nucl. Instr. and Meth. 9 (1960), 49.

D = 12.0 mm, s = 5.0 mm, and b = 3.0 mm. The field was mapped for five values of the source-to-puller distance d (5.0, 6.3, 7.5, and 10.0 mm) with two sets of measurements for each source: one set where the source was centered with respect to the puller slit (displacement a=0) and one set where the source was displaced from the center line of the slit by a = 1.5 mm to match the geometry with the curvature of the trajectories.

An enlarged scale of 10:1 was chosen for these measurements to get an accurate description of the field distribution for the computations. The shape of the ion-output slit (whose width is usually the order of 1 mm), the plasma boundary, and the influence of space charge were neglected. This neglection is more or less necessary since the mechanism of ion extraction from the arc plasma is not yet completely understood. What is known from observations in the case of extraction with a d.c. voltage is that the plasma boundary forms some sort of a meniscus whose actual shape depends on the geometry of the electrode arrangement, the ion density of the plasma and the extraction voltage[12]; the shape of the meniscus may be concave and thus provide some focusing or it may be convex, i.e., penetrate through the output slit of the source into the acceleration gap, and hereby produce a defocusing field distribution. If the extracting voltage is constant one can easily optimize the arc conditions

---

12) See for example J. Kistemaker, Nucl. Instr. and Meth. <u>11</u> (1961), 179.

and the geometry to get a focusing plasma boundary. However, if the ion extraction is accomplished with r.f. voltage, as is the case in the cyclotron, the situation is much more complicated and it is questionable whether one can apply the simple picture of the d.c. case. It is more likely that the plasma boundary at the output slit is pulsating, i.e., moving back and forth as the voltage changes, and at best there may be a focusing shape at one particular moment of the oscillation period. Whatever the true situation may be, if the width of the output slit is small, the distortions of the field produced by the edges of the slit and the instantaneous shape of the plasma boundary represent only a minor correction of the general potential distribution in the source-to-puller region.

From the measurements themselves only a few typical results will be shown. Equipotential lines for some cases are indicated in Figs. 4, 5, 6, 7, and 9 of the next section. The potential distributions between ion source and puller, measured along the x axis for the four values of distance d with the source in center position (a=0), are plotted in Fig. 2 for the circular source and in Fig. 3 for the square source. The straight curve in both figures shows the uniform-field potential which one would have in the case of two parallel plates a distance d apart. As one expects, the electric field penetrates to some extent into the puller slit, the fraction of the potential drop within the slit becoming larger if the spacing d is reduced. In the first half of the gap (i.e., at the side of the ion source) the electric field produced by the circular source is stronger than it would be in the uniform-field situation (Fig. 2). The square source, on the other hand, produces a field which in this region is fairly linear and matches rather close with the uniform-field case (Fig. 3). This picture changes slightly if the ion source is displaced from the center line by $a = 1.5$ mm: in the circular-source case the nonuniformity is increased and the field configuration becomes asymmetric (see Fig. 5) while the situation in the case of the square source remains practically the same.

3. Computational Results.

The numerical calculations of the trajectories in the field between source and extractor electrode were carried out with the Cartwheel Code[13] which integrates the equations of motion by the Runge-Kutta process. A great number of computer runs were made for different source-to-puller geometries and operating conditions. Since the characteristic features were basically very similar in all of these cases only the runs with a source-to-puller spacing of 6.3 mm will be discussed here, namely: (1) first-harmonic acceleration of protons, and (2) a typical example of second- and third-harmonic acceleration.

---

13) T. I. Arnette, H. G. Blosser, M. M. Gordon and D. A. Johnson, Nucl. Instr. and Meth. 18-19 (1962), 343.

3.1 First-Harmonic Acceleration.

For the dee voltage $U = U_o \cos(\theta_o + \omega_e t)$ a value of $U_o = 70$ kV was chosen as planned for the MSU cyclotron[8]; the magnetic field was $B_o = 13{,}774$ G corresponding to an electric frequency $f_e = 21$ Mc/s.

The first case in Fig. 4 shows the equipotential lines and a family of trajectories, starting with zero initial momentum, in the phase interval $-90^\circ \leq \theta_o \leq 60^\circ$, with the circular source in centered position. It is seen that in this case most of the ions are hitting the extractor electrode because of the curvature of the trajectories. With the ion source displaced from the center line by 1.5 mm, the trajectories are still very similar to the first case, except that now the favorable group of particles is not intercepted by the extractor electrode (Fig. 5). This favorable group of ions originates in the starting-phase interval from -90° to 30° and is well bunched radially due to a rather uniform energy gain. Beyond $\theta_o = 30^\circ$ the situation deteriorates very quickly: because of the rapidly decreasing instantaneous voltage particles starting in this phase interval gain less and less energy, and if they start at 60° or later, they are even decelerated again and hit the ion source near the output slit.

The pictures in Figs. 4 and 5 demonstrate how the starting phase and the rapid change of the instantaneous voltage influence the motion of particles leaving the ion source at the same point. The next figure shows the effects due to the geometry of the field configuration. The trajectories in this figure belong to particles starting at the same phase $\theta_o = -20^o$, but at different points of the source and with different momenta. At each of the five equidistant points between $x = -1.0$ mm and $x = 1.0$ mm three particles are starting with momenta $p_{x1} = -0.5 \times 10^{-4}$, $p_{y1} = 0.5 \times 10^{-4}$, $p_{x2} = 0.707 \times 10^{-4}$, $p_{y2} = 0$, $p_{x3} = 0.5 \times 10^{-4}$, $p_{y3} = 0.5 \times 10^{-4}$, respectively. These values are in units of $m_o c$ and correspond with an energy of about 2.3 eV which is the order of what one expects for ions leaving an arc plasma. Fig. 6 shows that while the trajectories of the three particles starting at the same point differ only slightly from one another, the "beam" as a whole is strongly defocused. The central part, for example, starting in an interval of 1 mm is spread to more than 3 mm as it passes through the extractor slit. The small difference of the three trajectories emerging from the same point can be explained by the fact that their initial energy is extremely small compared with the strength of the electric field, and as a result, these particles are practically following the direction of the field lines at the beginning despite different initial momenta. Because of the nonuniformity of the electric field at the ion source this effect causes an immediate beam divergence which extends into the second part of the gap, although here the particles are at high energy and less effected by field components normal to their trajectories.

In the case of the flat source (displaced by 1.5 mm from the center line of the puller) the field is almost uniform in the first half of the gap (Fig. 7). The trajectories of particles with different starting phases, however, are very similar to those in Fig. 5. The main difference is that the 60° particle returns earlier because the field strength and hence the initial energy gain near the flat source are smaller than in the circular-source case.

In Fig. 8 the kinetic energy of the ions and the transit angle $\tau = \omega_e t$ at three distances from the source, $x = d = 6.3$ mm, $x = 7.0$ mm, and $x = 9.0$ mm, are plotted as a function of the starting phase θ_o. The particles starting near -20° experience the highest energy gain reaching a value of about 67 kV at $x = 9.0$ mm. The transit-time curves have a minimum at starting phases near -10° and are fairly flat over a large interval. The increase towards the phases close to -90° indicates a certain amount of phase bunching in this region, i.e., particles starting earlier need longer to reach a given point and hence the actual phase $\theta = \theta_o + \tau$ at this point is not much different from the phase of particles that start later. For example, the group of particles leaving the source between -90° and -60° arrive at the line $x = 9.0$ mm at phases between -19° and -30°, respectively, i.e., they are bunched in time to a narrow pulse of only 11° length. In the starting-phase interval from -40° to 10°, however, the transit time is almost constant, indicating that no phase bunching occurs in this region of maximum-energy gain.

These results regarding energy gain and phase are only slightly effected by the geometric field distribution. The dominating factors are starting phase and transit time or distance traveled across the electric-field region. In this regard the behavior of the particles can very accurately be described by the uniform-field theory[14].

The influence of the field geometry is demonstrated by Fig. 9 where, as in Fig. 6, a group of particles starting at the same phase of -20° but at different points and with different momenta has been traced across the gap. The strong radial divergence of the previous circular-source case is here substantially reduced, the beam being almost parallel, with only a small amount of defocusing in the nonuniform field inside the extractor slit.

The flat source is of course not the ultimate. Further improvement of the beam optics is possible by recessing the source face at the output slit to form some sort of a Pierce type geometry[15]. With a slight angle of 10° a very favorable parallel-beam situation has been achieved in Fig. 10. To simplify the picture only the central rays (injection angle 0°) have been drawn. A larger angle of 30°, where the nonuniformity of the field is more localized near the output slit, results in a strong focusing effect (Fig. 11). This case is less desirable since it leads to a cross-over

---

14) M. Reiser, Nucl. Instr. and Meth. 18-19 (1962), 370.

15) J. R. Pierce, Theory and Design of Electron Beams, D. van Nostrand Co., Inc., New York, 1954.

which causes a beam divergence in the region beyond the extractor electrode.

3.2 Second- and Third-Harmonic Acceleration.

The dee voltages U_o used in the computer runs for the second-harmonic (N=2) and third-harmonic (N=3) modes were chosen to match the situation in the MSU cyclotron for constant orbit geometry[8], namely: U_o = 56.6 kV for N= 2 and U_o = 37.7 kV for N=3. The magnetic field and the electric frequency were the same as in the N=1 mode. The two runs to be discussed here were made with the field of the flat source, the source-to-puller spacing being again 6.3 mm.

Fig. 12 shows the trajectories for several particles with different starting phases in the case N=2 (deuterons); in Fig. 13 the corresponding transit-angle and kinetic-energy curves are plotted. The situation is qualitatively similar to the proton case in Figs. 7 and 8; however, as one expects for the higher-harmonic mode, the transit angle τ is larger and the starting phase for maximum energy gain is about -30^o instead of -20^o for the protons. At the line x = 9.0 mm, for example, the kinetic energy gain for the favorable starting phase of -30^o is 53.5 keV, i.e., 94.5% of the possible maximum gain of 56.6 keV under d.c. conditions, as compared to 95.7% (67 keV out of 70 keV) in the N=1 case. The minimum transit angle at this line is 51^o compared to 32.5^o in the previous case.

This general trend towards larger transit angles at higher-harmonic modes continues if one turns to the case N=3 ($_{12}C^{4+}$): The particle leaving the source at a phase of 30° (decreasing instantaneous voltage), for example, is initially accelerated but then loses energy on its way to the puller slit and almost hits the puller structure; the 60° particle, on the other hand, is immediately turned back to the source as it comes into the decelerating half period of the r.f. field. (Fig. 14). The favorable starting phase is now -45°, the maximum energy gain at the line $x = 9.0$ mm about 92% and the minimum transit angle at this line 77.5° (Fig. 15).

4. Conclusions.

The results of these initial-motion studies demonstrate the great influence of the electric-field configuration in the immediate neighborhood of the ion source. With respect to radial focusing the actual shape of the source structure is far more important than that of the extractor electrode, the reason being that at the start the particles practically follow the direction of the electric field lines due to their small energy, while they are much "stiffer" and hence less manageable as they pass through the puller slit. The strong defocusing effect in the case of a cylindrical arc chamber can be reduced substantially if a flat source is used, and the ideal condition of a parallel beam can be obtained by slightly recessing the source face at the output slit. With a recessed source face one could also compensate the defocusing effects of space charge and a convex plasma boundary, both of which were neglected in these studies, the optimum geometry probably being somewhere between the cases of Figs. 10 and 11. These results are basically also applicable to the vertical motion, which was not studied in the program. Here, too, it should be possible to provide sufficient focusing by properly shaping the source structure at the output slit, while the actual shape of the puller slit is less important. The final picture is then a source structure which is flat at the side facing the extractor electrode and recessed at the output slit with an angle of about 20° in both radial and vertical directions.

5. Acknowledgements.

The author would like to thank W. Schreiner, who carried out the conducting-paper measurements, prepared the field data for the computer, and plotted the results. The assistance of T. I. Arnette, who guided the computer runs, is gratefully acknowledged.

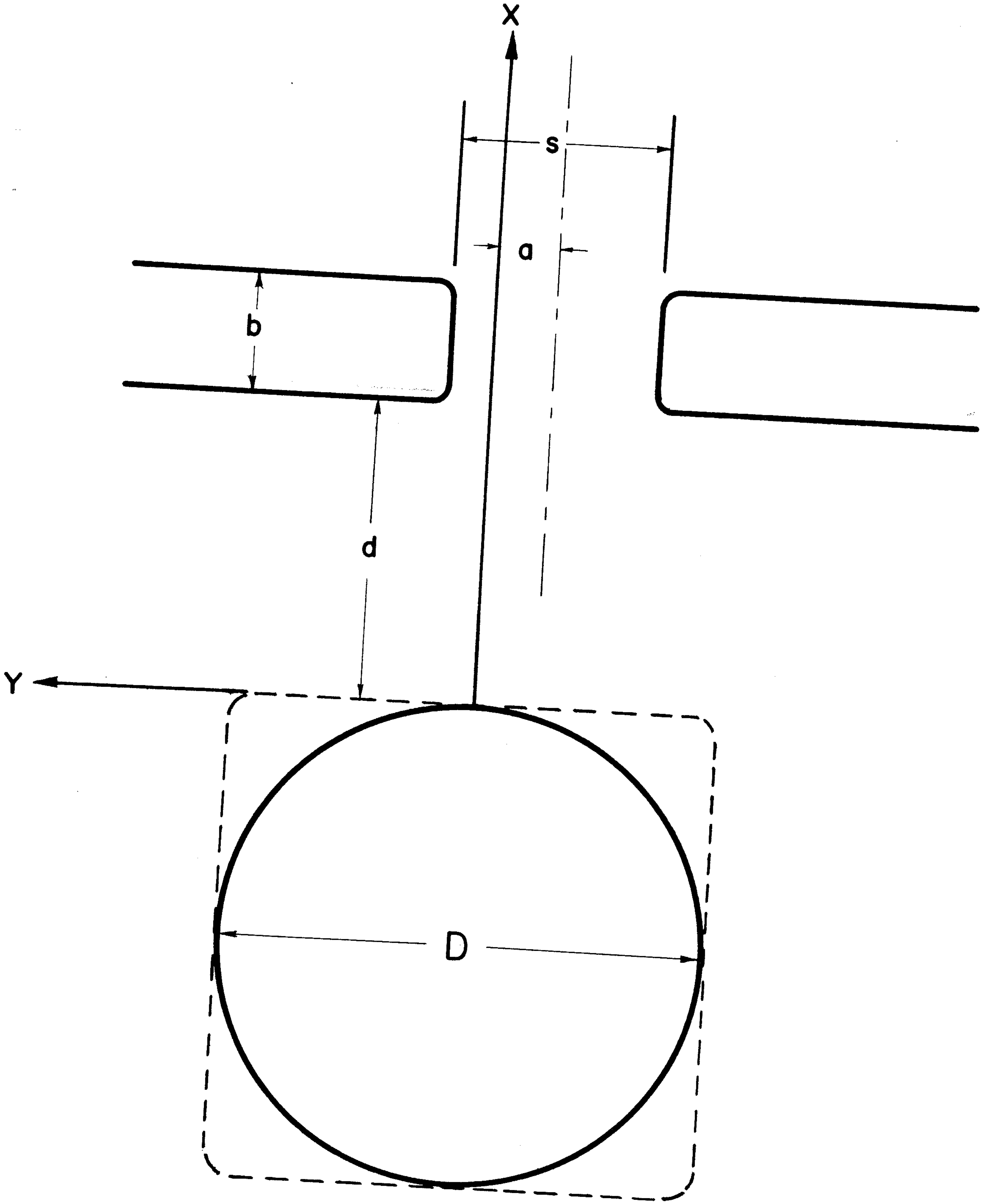

Fig. 1: Source-puller geometry for the electric-field measurements.

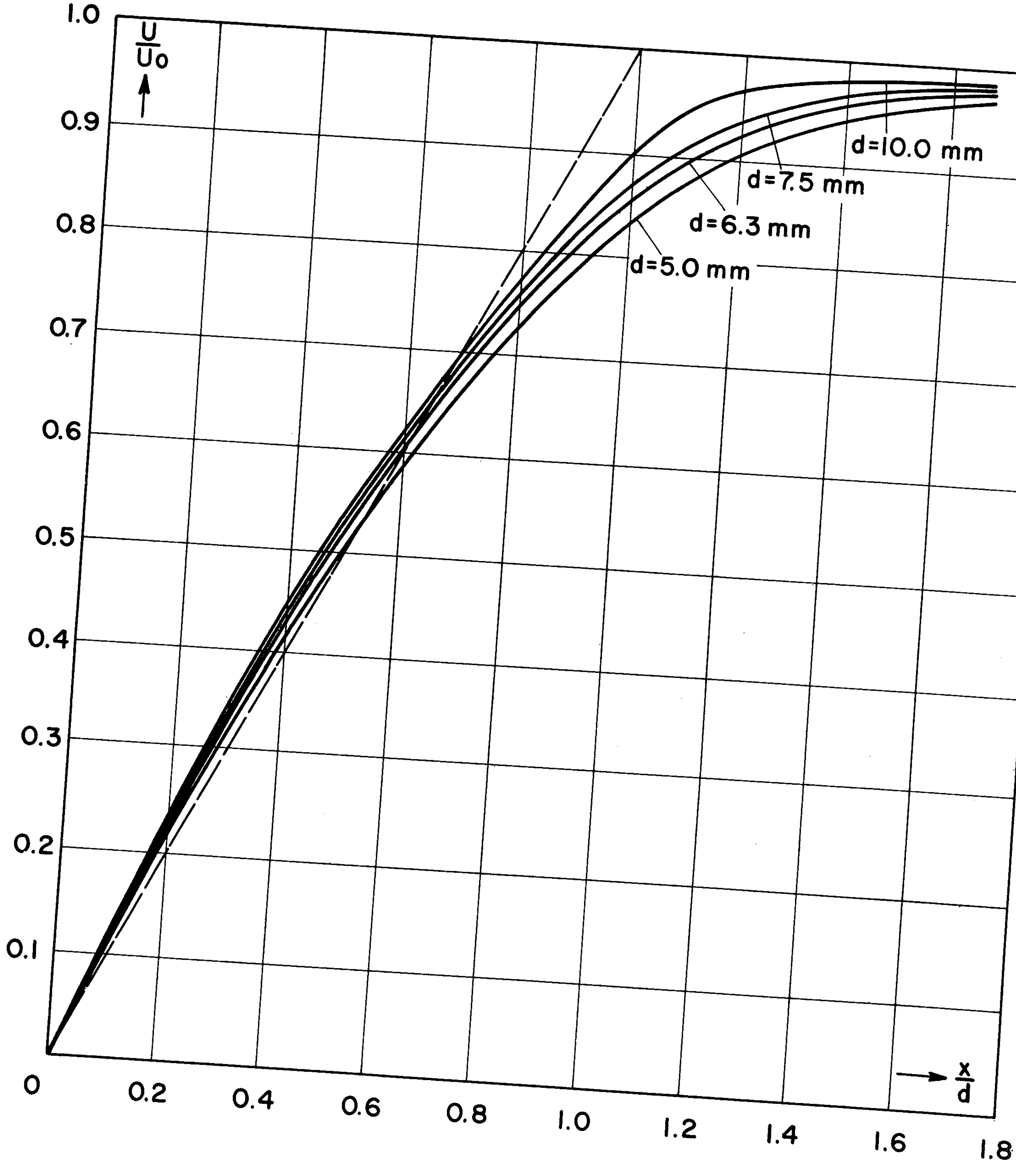

Fig. 2: Potential distributions in the case of the circular source in centered position.

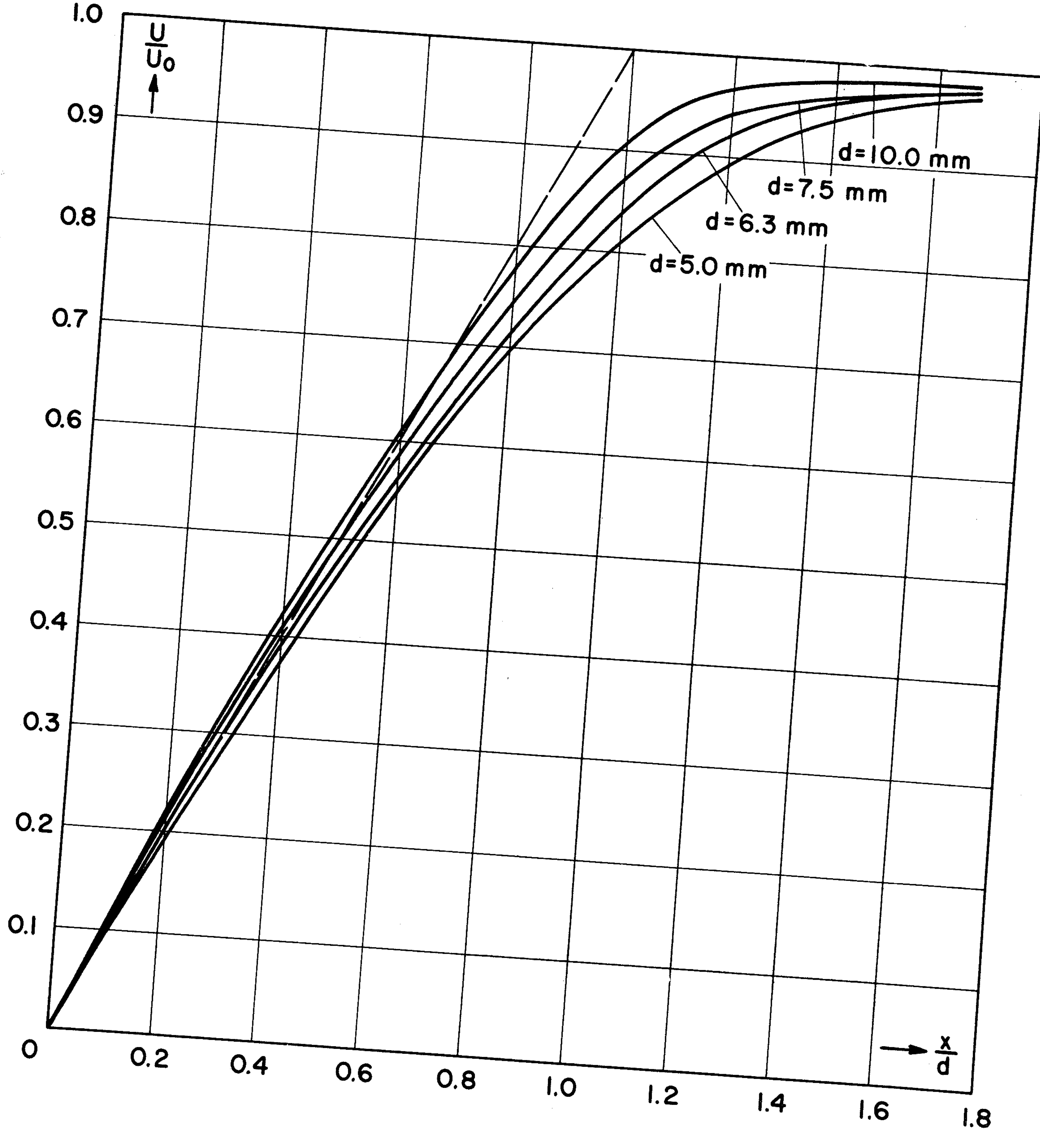

Fig. 3: Same as Fig. 2 for square source.

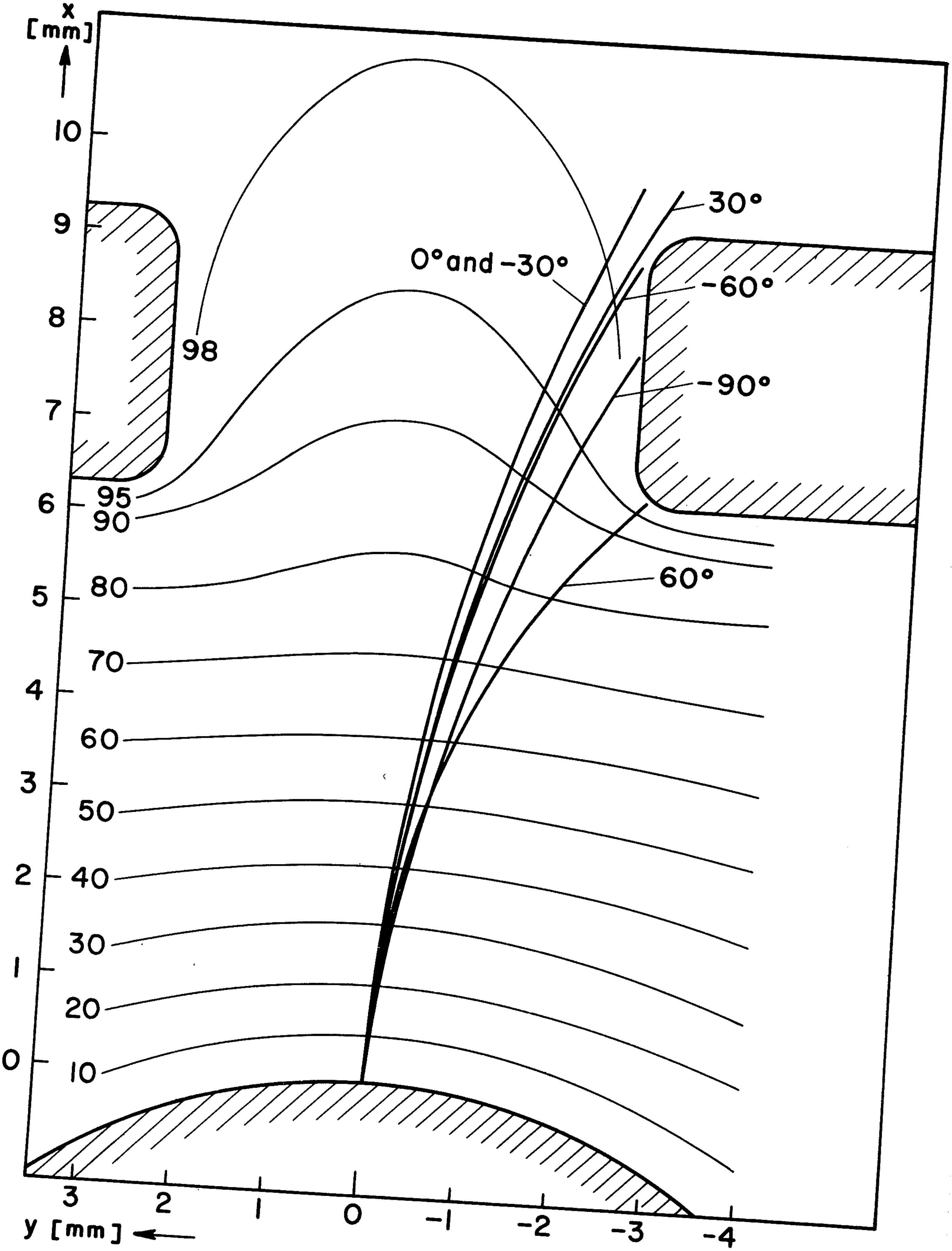

Fig. 4: Equipotential lines and proton trajectories with circular source in centered position (d = 6.3 mm).

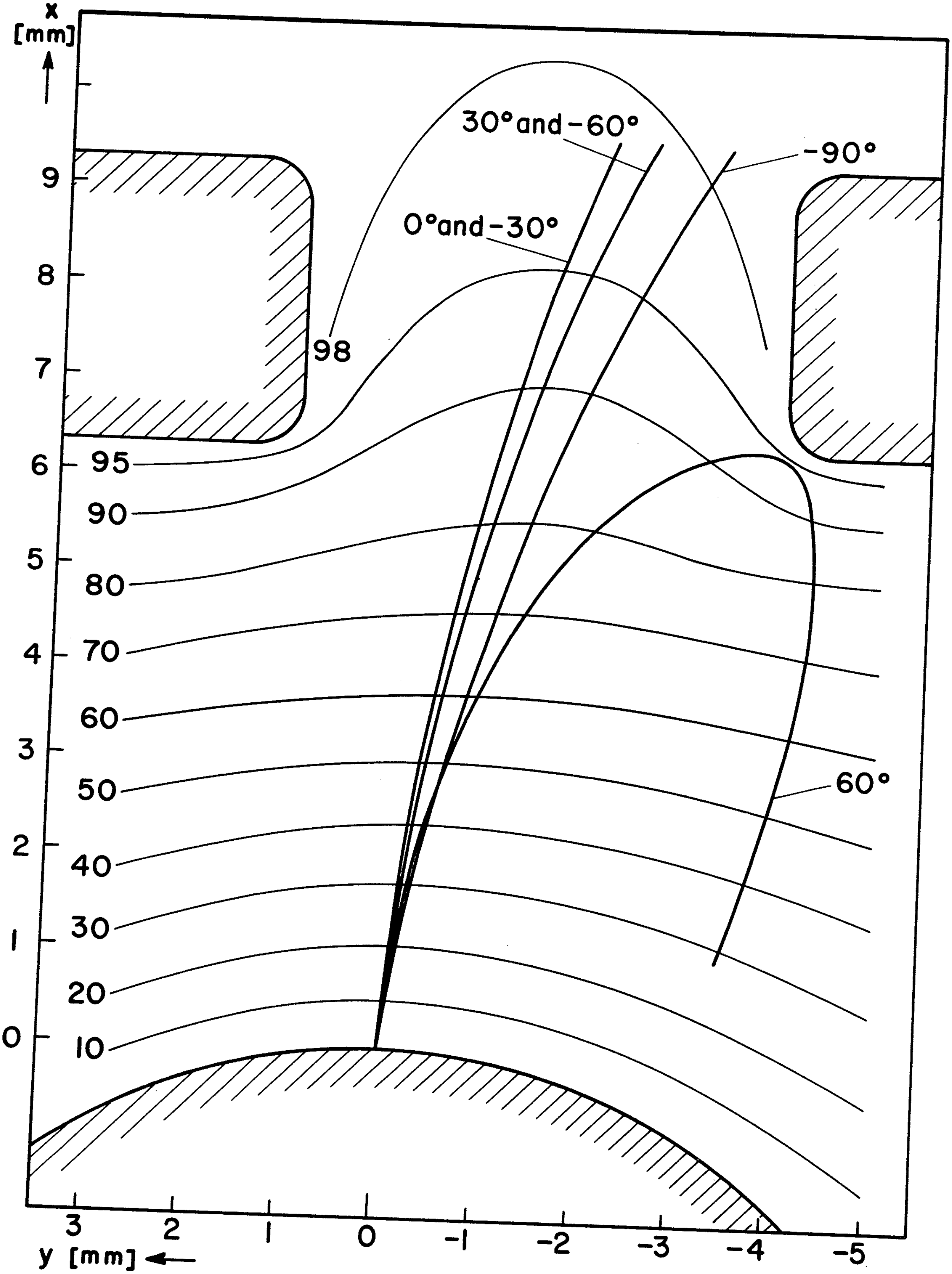

Fig. 5: Same as Fig. 4 with off-center source.

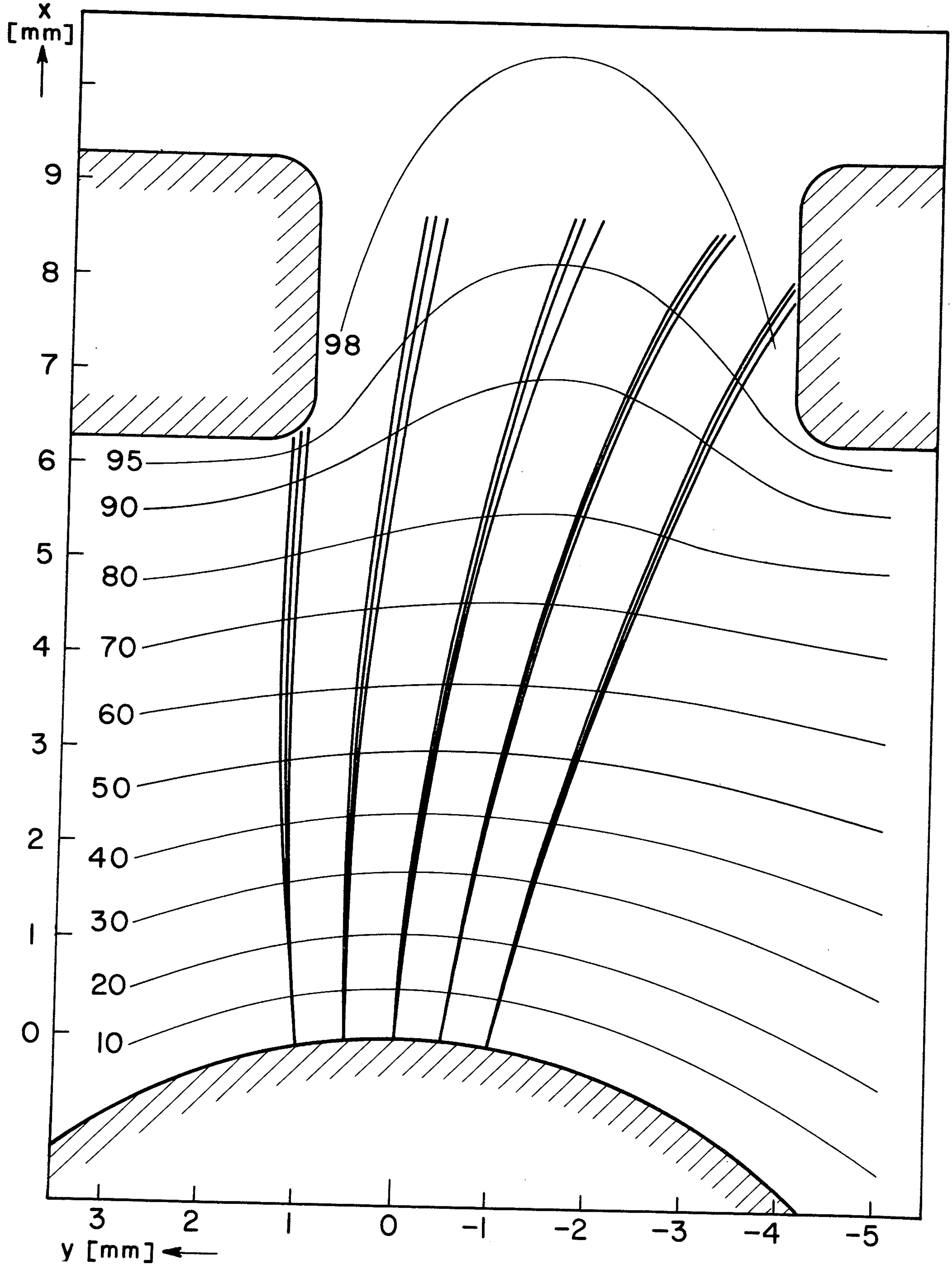

Fig. 6: Trajectories of protons starting at phase $\theta_o = 20^o$ with different initial conditions (circular source).

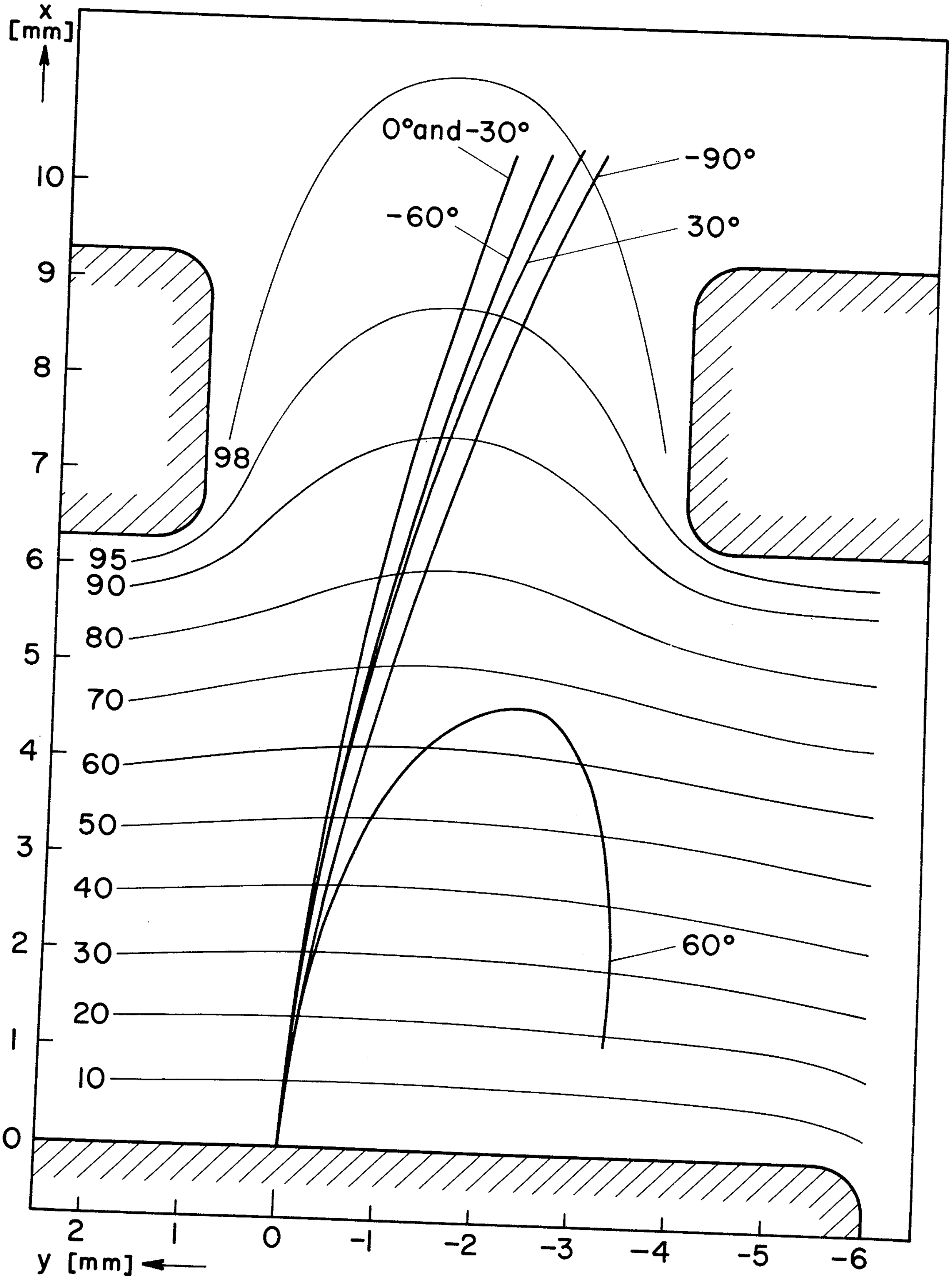

Fig. 7: Equipotentials and proton trajectories in the case of the square source.

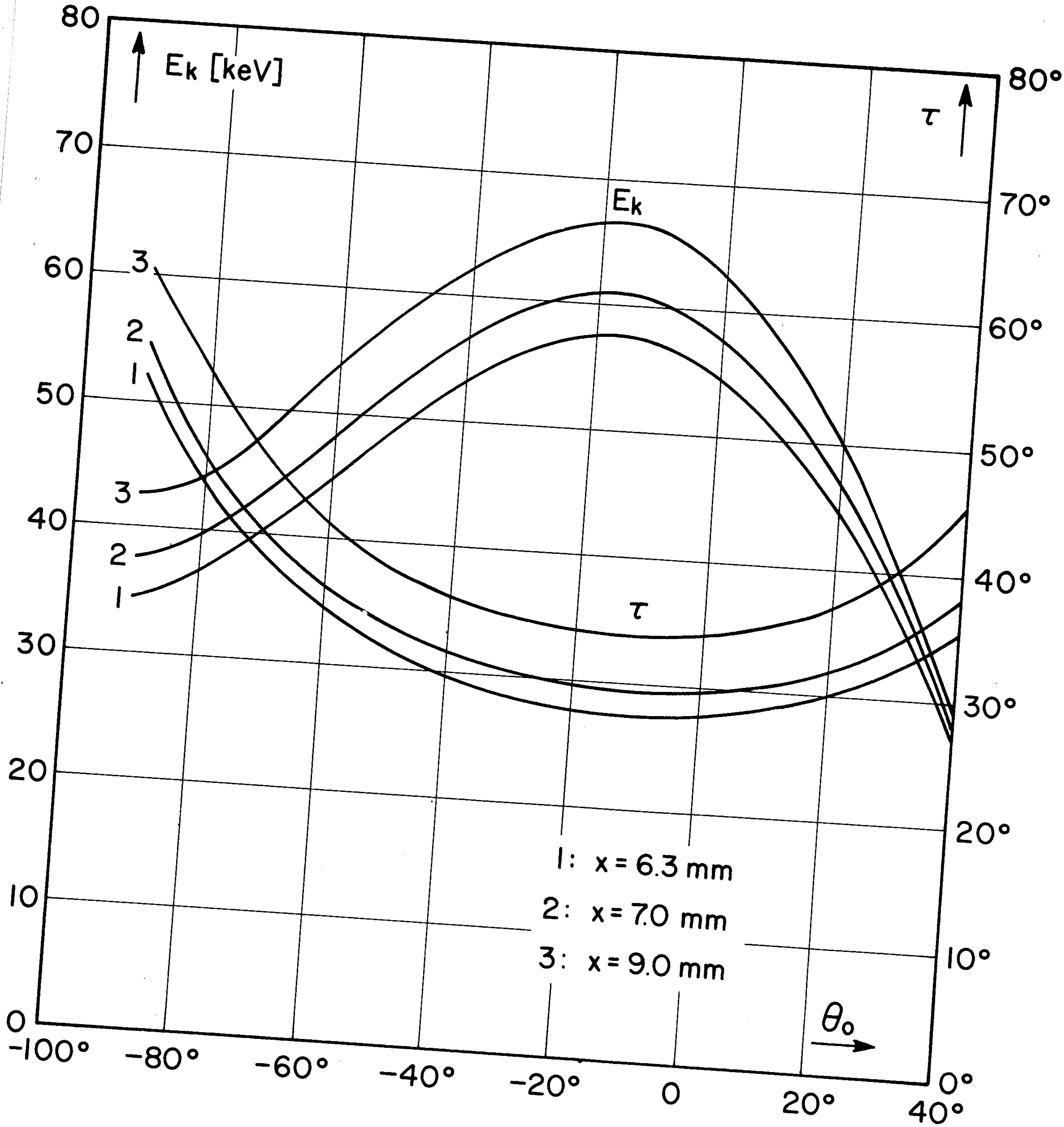

Fig. 8: Kinetic energy E_k and transit angle τ of the protons at three distances from the source as a function of starting phase θ_o (square source).

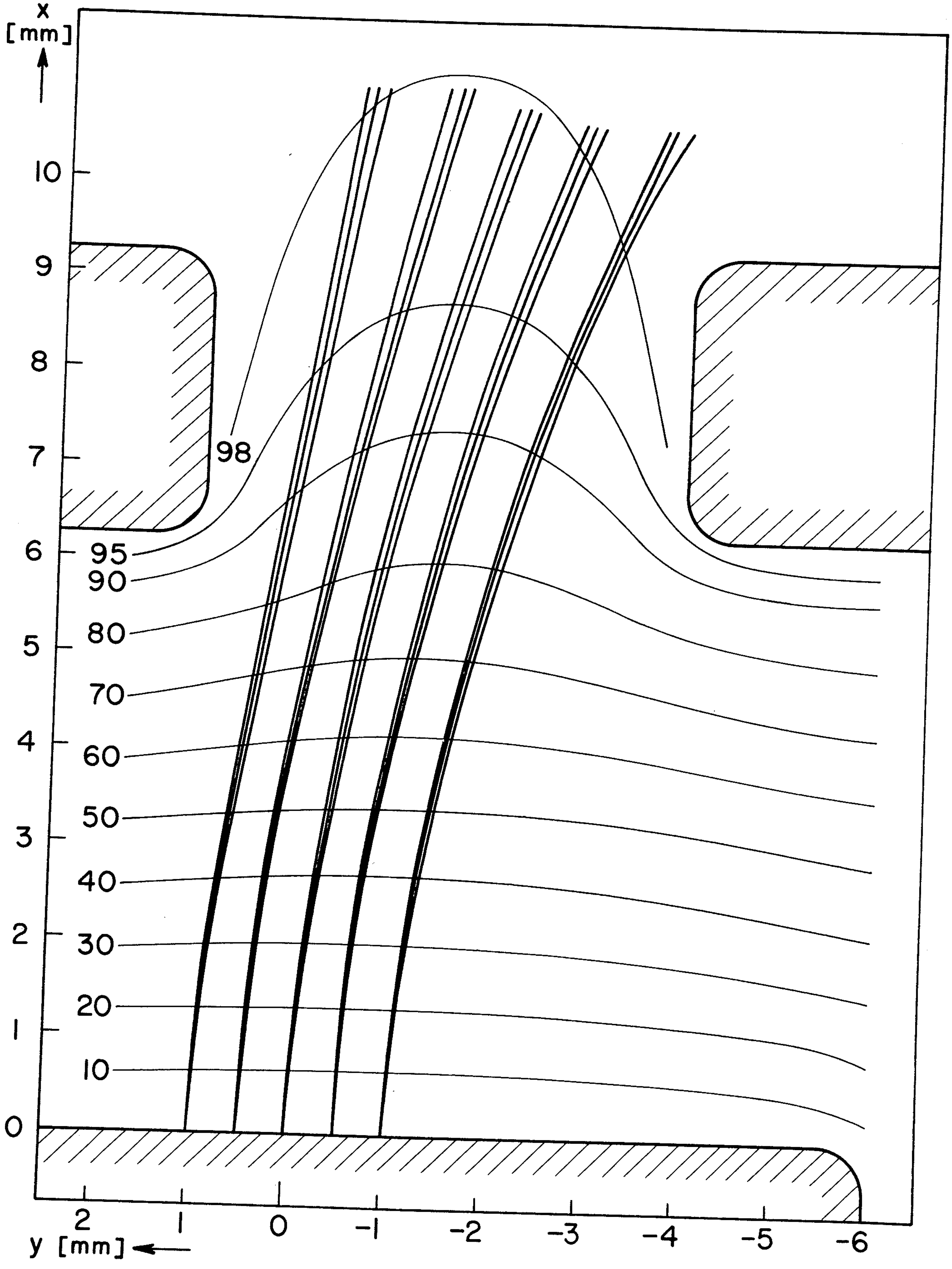

Fig. 9: Same as Fig. 6 with square source.

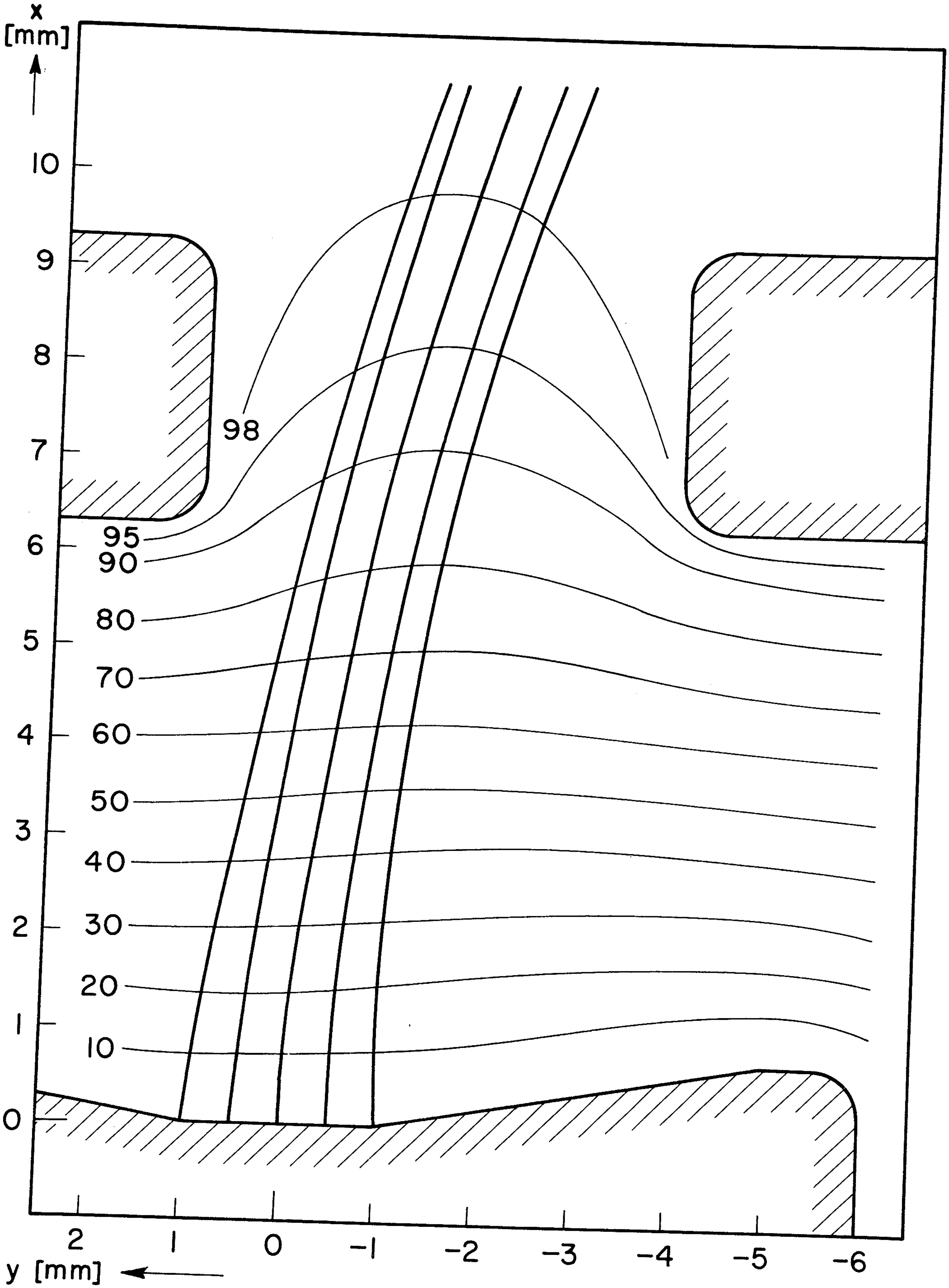

Fig. 10: Ideal focusing in the case of a slightly recessed source face (angle 10°).

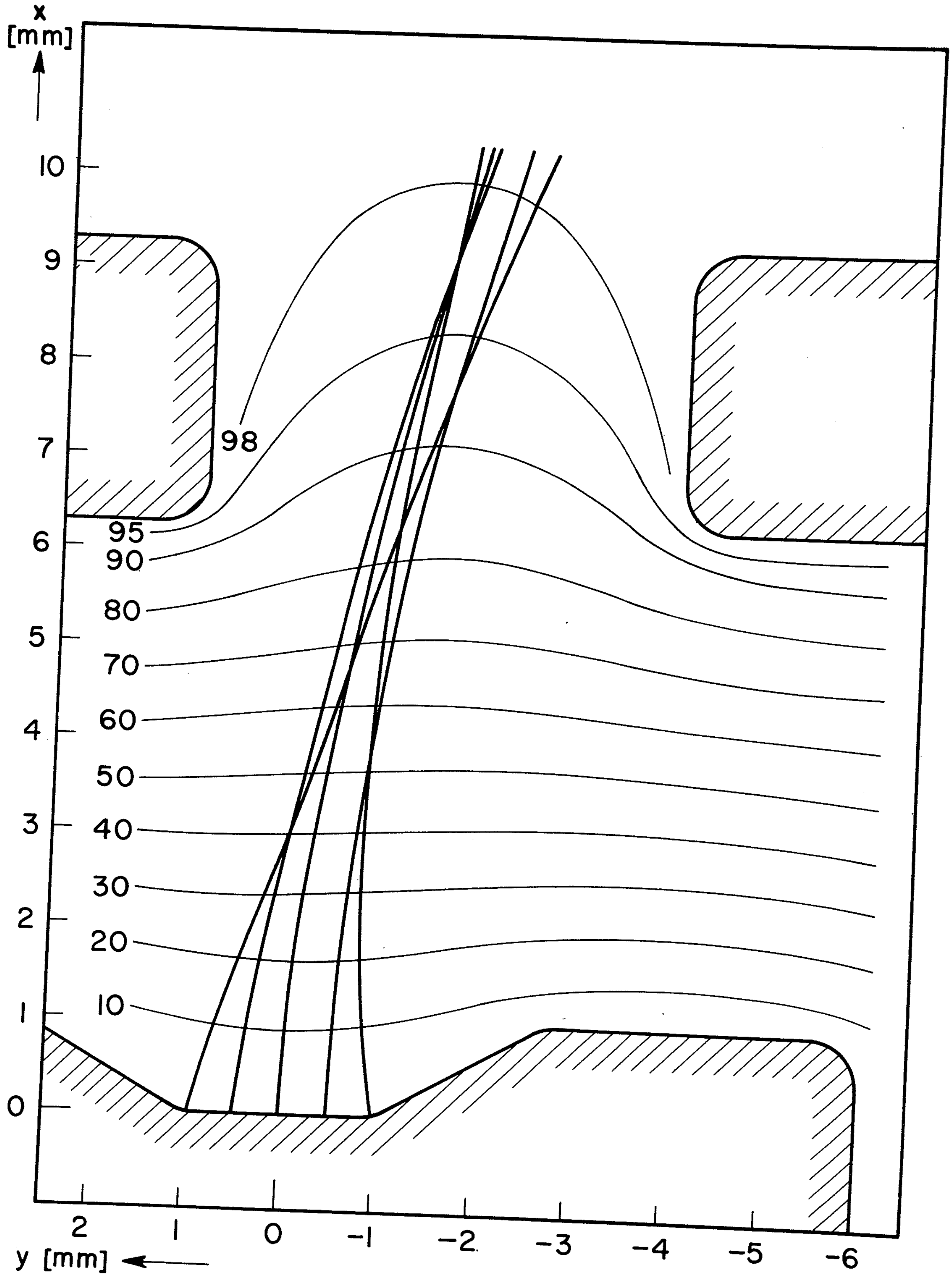

Fig. 11: Overfocusing in the case of a strongly recessed source face (angle 30°).

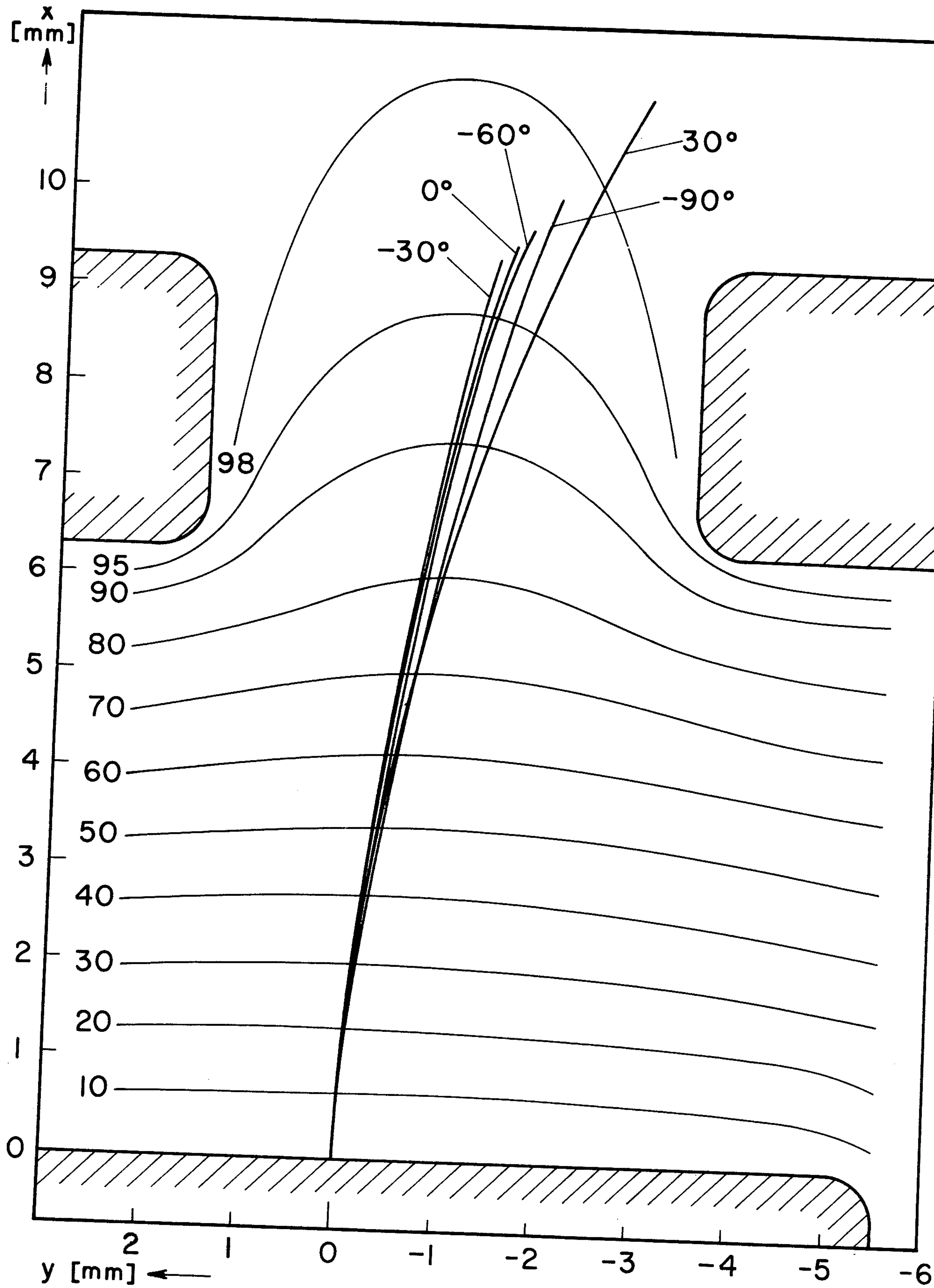

Fig. 12: Ion trajectories in the case of second-harmonic acceleration (N=2, deuterons).

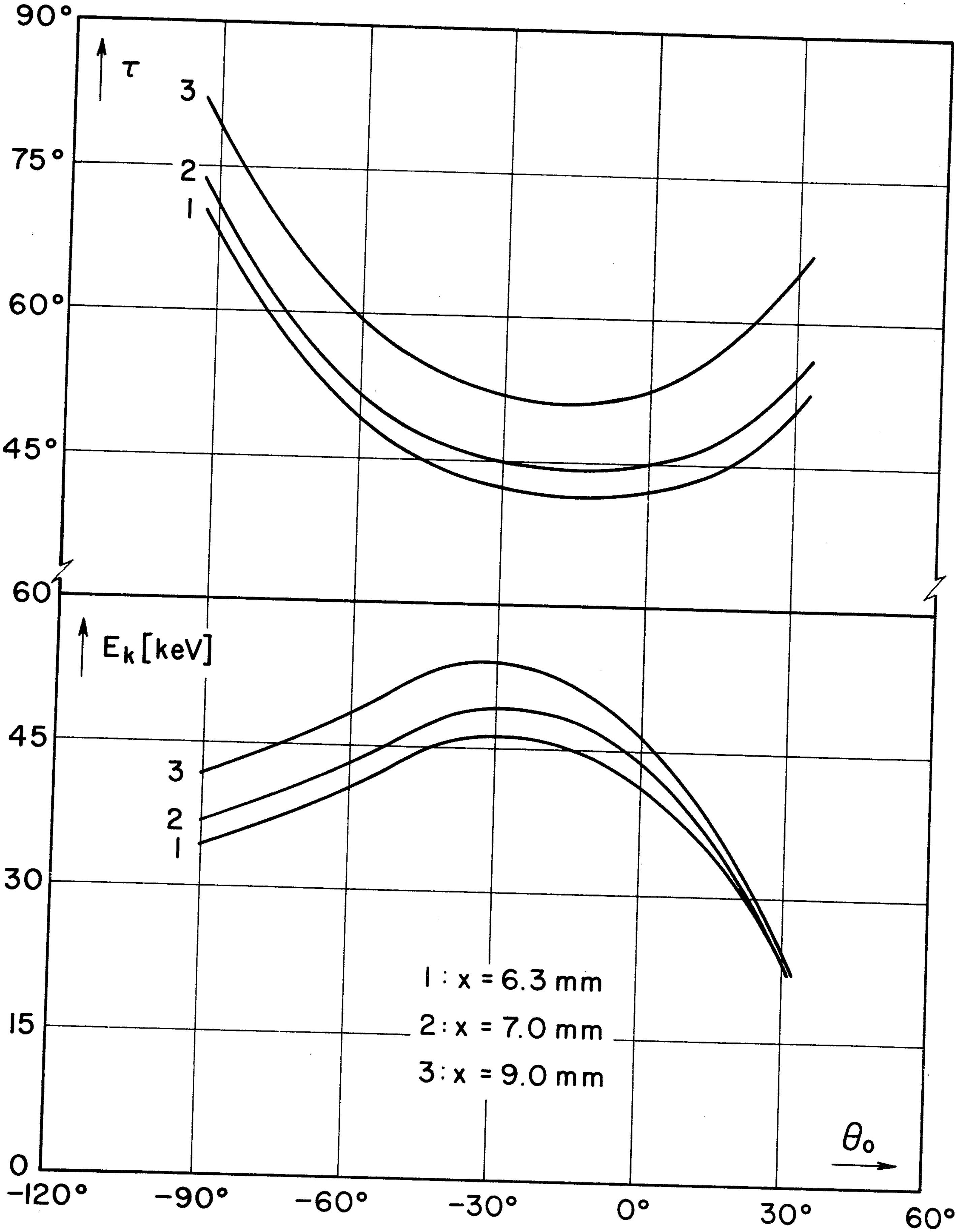

Fig. 13: Kinetic energy and transit angle at three distances from the source as a function of starting phase in the N=2 mode.

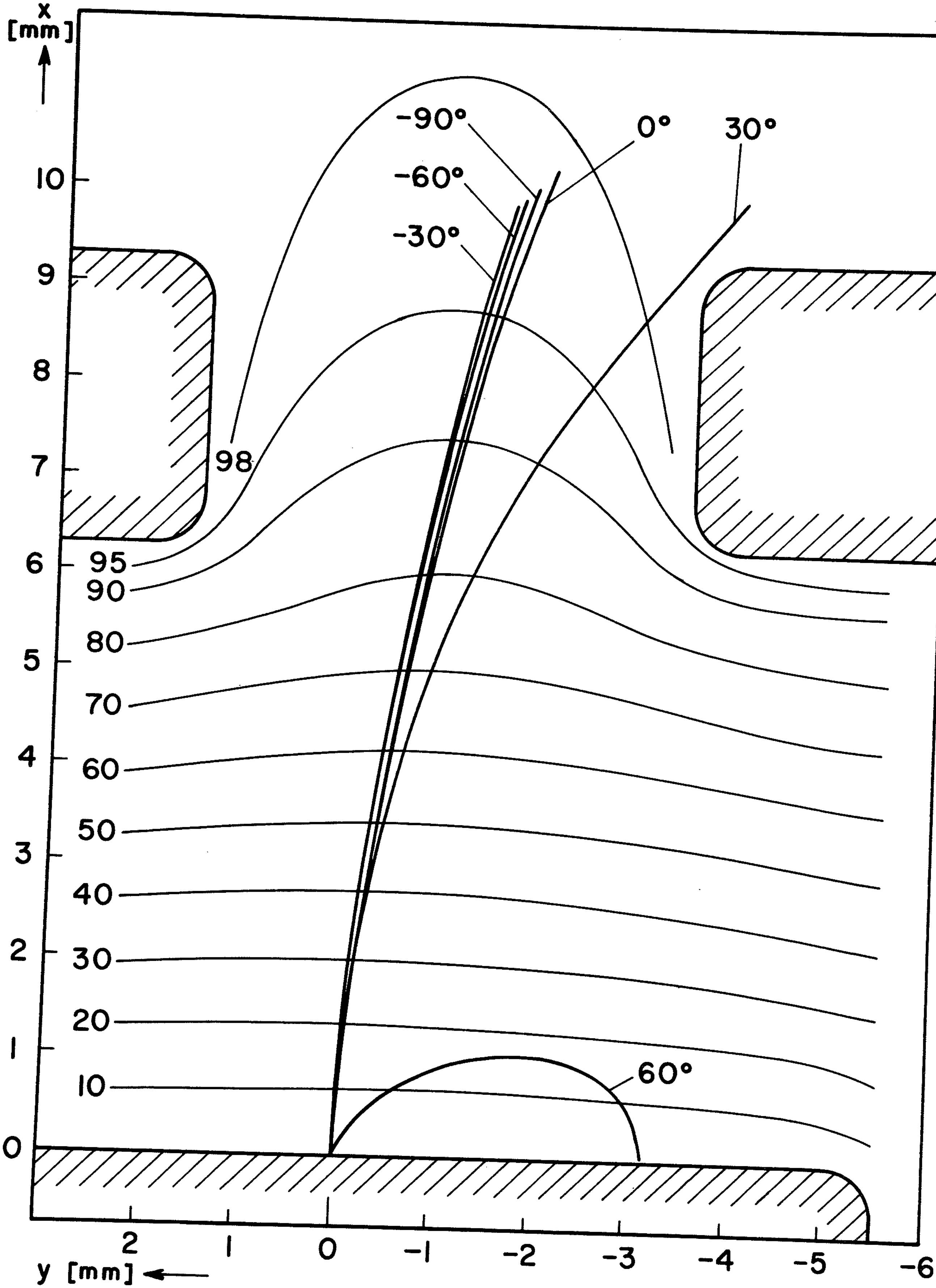

Fig. 14: Ion trajectories in the third-harmonic mode (N=3, $_{12}C^{4+}$).

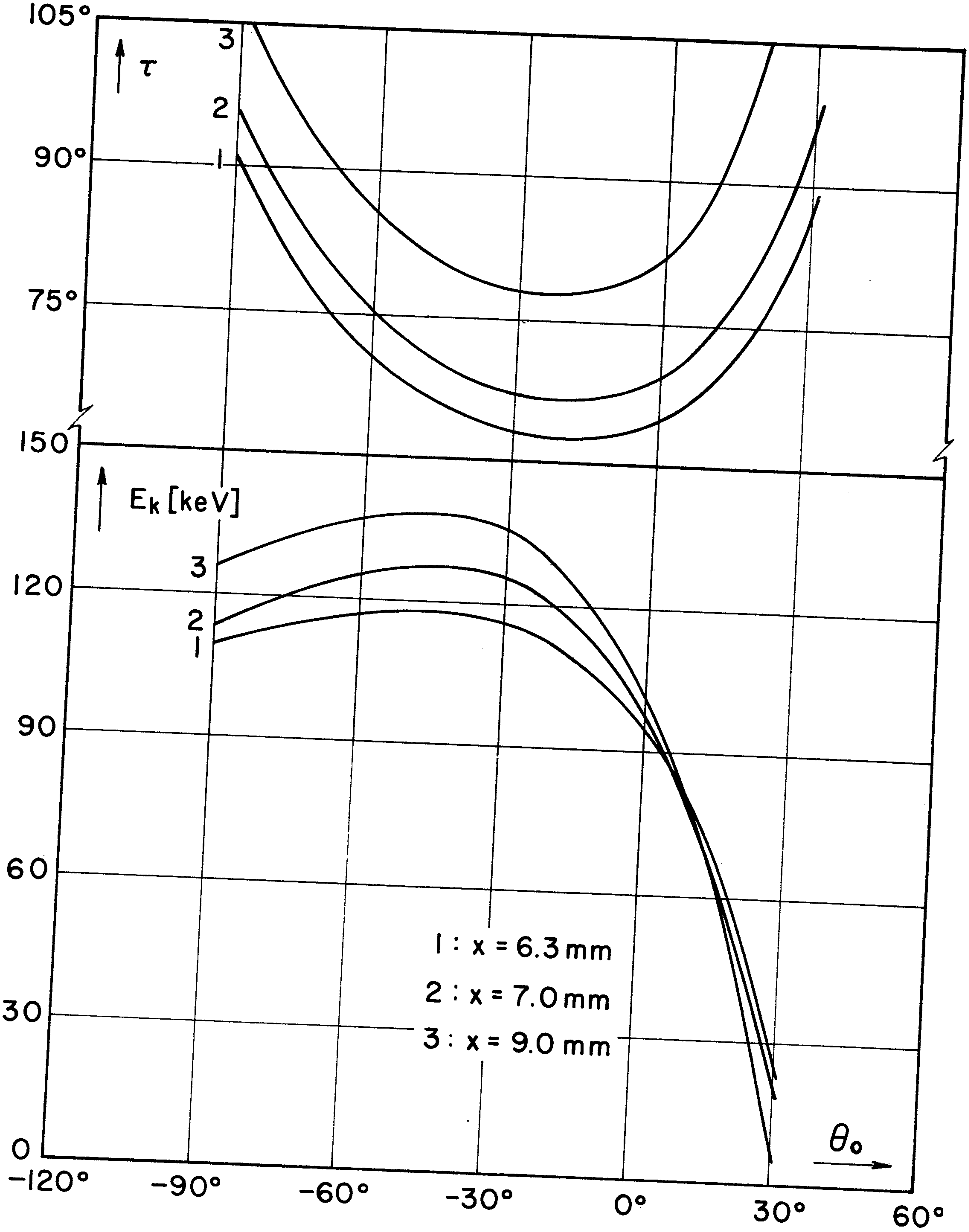

Fig. 15: Kinetic energy and transit angle in the N=3 mode.